# Unifying Magnons and Triplons in Stripe-Ordered Cuprate Superconductors

G. S. Uhrig,[1] K. P. Schmidt,[1] and M. Grüninger[2]

[1]*Institut für Theoretische Physik, Universität zu Köln, Zülpicher Straße 77, D-50937 Köln, Germany*

[2]*II. Physikalisches Institut, Universität zu Köln, Zülpicher Straße 77, D-50937 Köln, Germany*

(Received 26 February 2004; published 20 December 2004)

Based on a two-dimensional model of coupled two-leg spin ladders, we derive a unified picture of recent neutron scattering data of stripe-ordered $La_{15/8}Ba_{1/8}CuO_4$, namely, of the low-energy magnons around the superstructure satellites and of the triplon excitations at higher energies. The resonance peak at the antiferromagnetic wave vector $\mathbf{Q}_{AF}$ in the stripe-ordered phase corresponds to a saddle point in the dispersion of the magnetic excitations. Quantitative agreement with the neutron data is obtained for $J =$ 130–160 meV and $J_{cyc}/J = 0.2$–$0.25$.

DOI: 10.1103/PhysRevLett.93.267003 PACS numbers: 74.25.Ha, 75.10.Jm, 75.40.Gb, 75.50.Ee

Quantum magnetism in the cuprate superconductors is an intriguing issue. A detailed understanding of the dynamic spin susceptibility as measured by inelastic neutron scattering (INS) experiments should allow to clarify the role of magnetism in the mechanism of high-$T_c$ superconductivity. In particular two features have been in the focus of interest: the appearance of the so-called resonance peak [1,2] in the superconducting phase at the antiferromagnetic wave vector $\mathbf{Q}_{AF} = (1/2, 1/2)$ [see Fig. 1(b)] at finite energies [e.g., 41 meV in optimally doped $YBa_2Cu_3O_{7-\delta}$ (YBCO)] and the existence of stripe order which manifests itself in superstructure satellites around $\mathbf{Q}_{AF}$ [Fig. 1(b)] [2–4]. In general, these superstructure satellites are incommensurate. For many years, these two features have been regarded as separate issues, each of them apparent in only one of the two families of cuprates on which most neutron studies have focused: $La_{2-x}Sr_xCuO_4$ (LSCO) and YBCO. But recent experimental results show that the resonance peak in YBCO is accompanied at lower energies by incommensurate reflections [5–8], and that stripe order may appear also in YBCO [9]. Very recently, Tranquada *et al.* [10] observed a resonance peak at $\mathbf{Q}_{AF}$ also in stripe-ordered $La_{15/8}Ba_{1/8}CuO_4$ (for $T > T_c$).

An $S = 1$ collective mode (the resonance peak) in the superconducting phase is a prominent feature of many different theoretical scenarios. Its interpretation ranges from a particle-hole bound state (see Refs. in [1,2]) to a particle-particle bound state in SO(5) theory [11]. In the stripe-ordered phase the choice of the microscopic model is straightforward. Static stripe order corresponds to a segregation into hole-rich charge stripes and hole-poor spin ladders. Tranquada *et al.* [10] analyzed their INS data at high energies (including the resonance) in terms of the elementary triplet excitations (triplons [12]) of isolated *two-leg* ladders [Fig. 1(a)], which are realized in case of bond-centered stripes [13]. But the incommensurate low-energy excitations were described in a separate model as spin waves (magnons), motivated by the existence of weak long-range order.

Based on a model of coupled two-leg $S = 1/2$ ladders, we derive a unified description of the low-energy superstructure modes, of the resonance peak and of the high-energy excitations observed in Ref. [10]. The superstructure modes arise from a ferromagnetic coupling between neighboring ladders, whereas the resonance peak corresponds to a saddle point of the triplon dispersion. The central result is that we arrive at a quantitative agreement with the INS data for realistic values of the exchange parameters.

The ladders shown in Fig. 1(a) are described by a standard Heisenberg Hamiltonian (see, e.g., Ref. [14]) with rung coupling $J_\perp > 0$, leg coupling $J_\parallel > 0$, and by the four-spin operators of a cyclic exchange

$$H_{cyc} = J_{cyc} \sum_i [(\mathbf{S}_i^L \cdot \mathbf{S}_i^R)(\mathbf{S}_{i+1}^L \cdot \mathbf{S}_{i+1}^R) + (\mathbf{S}_i^L \cdot \mathbf{S}_{i+1}^L)(\mathbf{S}_i^R \cdot \mathbf{S}_{i+1}^R) - (\mathbf{S}_i^L \cdot \mathbf{S}_{i+1}^R)(\mathbf{S}_{i+1}^L \cdot \mathbf{S}_i^R)], \quad (1)$$

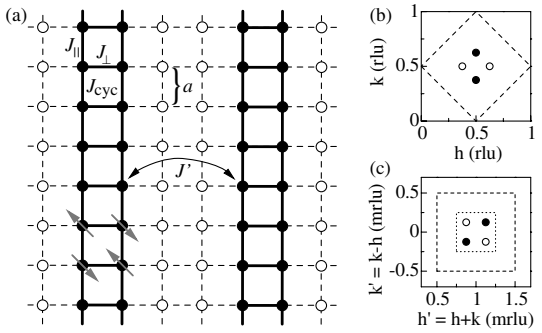


FIG. 1. (a) 2D square lattice split into two-leg $S = 1/2$ ladders (full dots) coupled by bond-centered charge stripes (open dots). (b) Momentum space, coordinates in reciprocal lattice units $2\pi/a$ (rlu). Dashed line: magnetic Brillouin zone around the antiferromagnetic wave vector $\mathbf{Q}_{AF} = (1/2, 1/2)$. Open (full) dots: superstructure peaks from vertical (horizontal) ladders. (c) Momentum space rotated by 45° with $h' = h + k$ and $k' = k - h$, thus $\mathbf{Q}'_{AF} = (1, 0)$ in magnetic reciprocal lattice units $2\pi/\sqrt{2}a$ (mrlu). Dotted line: see caption of Fig. 4.

 

where $i$ counts the rungs, and $R$ and $L$ label the two legs. Inclusion of $J_{\rm cyc} \approx 0.2$–$0.25$ is crucial in order to obtain quantitative agreement with experimental data, both in two-leg ladders [15] and in the 2D cuprates [16,17]. The ferromagnetic (FM) interladder coupling $J' < 0$, see Fig. 1(a), is an effective coupling which results from integrating out the degrees of freedom in the stripes. If two spins on adjacent ladders interact via a stripe rung with only one spin, they prefer to be antiparallel to this spin, giving rise to an effective FM coupling. The interaction via a half-filled stripe rung (two spins) implies an antiferromagnetic (AFM) coupling. Plausibly, the more direct FM coupling via one spin exceeds the AFM coupling via two spins, so that a weak average FM coupling results.

We start from an effective model for isolated ladders which we have determined previously by perturbative CUTs (continuous unitary transformations) [14,18]. The effective model is computed perturbatively to the order $n = 10$, which means that processes over a distance of up to ten rungs are taken into account. The one-triplon part is $H_{\rm ladder} = \sum_{k,\alpha} \omega_k^0 t_k^{\alpha,\dagger} t_k^\alpha$, where the operator $t_k^{\alpha,\dagger}$ ($t_k^\alpha$) creates (annihilates) a hard-core boson—a triplon [12]—with spin $S = 1$, momentum $k$, and one of the three triplet flavors $\alpha \in \{x, y, z\}$. The dispersion $\omega_k^0$ [Fig. 2(a)] is obtained as a series in $J_\parallel/J_\perp$ and $x_{\rm cyc} = J_{\rm cyc}/J_\perp$ and evaluated by extrapolation [14,19]. To describe the square lattice we focus on $J_\parallel = J_\perp$ where the extrapolation is reliable [14]. Inclusion of $J_{\rm cyc}$ reduces $\omega_k^0$ and, in particular, the gap at $k = 1/2$ (by 50% for $x_{\rm cyc} = 0.2$).

We use the unitary transform of the observables $S_i^{\alpha,{\rm R/L}}$

$$S_{i,\rm eff}^{\alpha,\rm R} := U^\dagger S_i^{\alpha,\rm R} U = \sum_\delta a_\delta (t_{i+\delta}^{\alpha,\dagger} + t_{i+\delta}^\alpha) + \ldots \quad (2)$$

where the dots stand for normal-ordered quadratic and higher terms in the bosonic operators. On the level linear in bosonic operators, $S_{i,\rm eff}^{\alpha,\rm L} = -S_{i,\rm eff}^{\alpha,\rm R}$ holds since rung triplets are odd excitations relative to rung singlets with respect to reflection about the centerline of the ladder. The

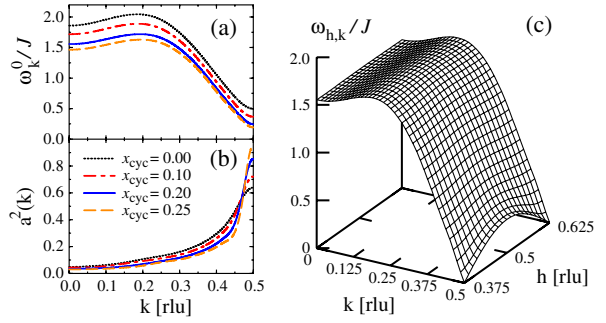


FIG. 2 (color online). (a), (b): dispersion $\omega_k^0$ and spectral weight $a^2(k)$ of one triplon in a two-leg $S = 1/2$ ladder with $J_\parallel = J_\perp = J$ and $x_{\rm cyc} = J_{\rm cyc}/J_\perp$. (c) One-triplon dispersion $\omega_{h,k}$ for coupled ladders at the quantum critical point $J'/J = -0.072$ for $x_{\rm cyc} = 0.2$.

Fourier transform of Eq. (2) yields

$$S(k)_{\rm eff}^{\alpha,\rm R} = a(k)(t_k^{\alpha,\dagger} + t_{-k}^\alpha). \quad (3)$$

Below we only need the one-triplon weight $a^2(k)$ [Fig. 2(b)], which is extrapolated in the same way as $\omega_k^0$. Relative to the total weight $(S_i^\alpha)^2 = 1/4$ of the local operator $S_i^\alpha$, the $k$-integrated one-triplon weight $\int_0^1 a^2(k)dk$ is 74% [18], 70%, 63%, and 59% for $x_{\rm cyc} = 0$, 0.1, 0.2, and 0.25, respectively. The missing weight belongs to multitriplon channels. By inclusion of $J_{\rm cyc}$, $a^2(k)$ becomes more pronounced around $k = 1/2$.

The key idea is to couple neighboring ladders weakly by $J'$ [see Fig. 1(a)]:

$$H' = -J' \sum_{h,k;\alpha} d_{h,k}(t_{h,k}^{\alpha,\dagger} + t_{-h,-k}^\alpha)(t_{h,k}^\alpha + t_{-h,-k}^{\alpha,\dagger}), \quad (4)$$

where $d_{h,k} := \cos(8\pi h) a^2(k)$ and $h$ is the wave vector perpendicular to the ladders measured in reciprocal lattice units (rlu) of the square lattice; cf., Figure 1. The total Hamiltonian $H$ is the sum of $H_{\rm ladder}$ for all ladders and $H'$. Since $J' \ll J$ it is justified to neglect the hard-core constraint so that a Bogoliubov transformation yields $H = \sum_{h,k;\alpha} \omega_{h,k} t_{h,k}^{\alpha,\dagger} t_{h,k}^\alpha$ with

$$\omega_{h,k} = \sqrt{(\omega_k^0)^2 - 4J' d_{h,k} \omega_k^0}. \quad (5)$$

In the INS data [10] the minima are at $h = 1/2 \pm 1/8$, in agreement with a ferromagnetic $J' < 0$.

We intend to describe the physics at the quantum critical point where magnons just emerge [20], i.e., we choose $J'$ such that $\omega_{h,k} = 0$ at the minima. The corresponding values for $J'$ are $-0.20$, $-0.13$, $-0.072$, and $-0.051$ for $x_{\rm cyc} = 0$, 0.1, 0.2, and 0.25, respectively. This is a physically plausible range [21]. The overall shape of the 2D dispersion $\omega_{h,k}$ is depicted in Fig. 2(c). Magnons with linear dispersion emerge from $(1/2 \pm 1/8, 1/2)$. At $\mathbf{Q}_{\rm AF} = (1/2, 1/2)$ a saddle point occurs. The dispersion at higher energies is hardly changed from its form for isolated spin ladders. This stems from the quadratic average (5) and from the suppression of the one-triplon hopping for smaller values of $k$ due to the factor $a^2(k)$; cf., Figure 2(b).

The one-triplon part of the dynamic structure factor $S_{h,k}(\omega)$ reads

$$S_{h,k}(\omega) = -\frac{2}{\pi} {\rm Im} \frac{\sin^2(\pi h) a^2(k) \omega_k^0}{(\omega + i0_+)^2 - \omega_{h,k}^2} \quad (6)$$

where $a^2(k)$ stems from (3), the factor $\sin^2(\pi h)$ from the interference of the two spins on a single rung, and $\omega_k^0$ from the Bogoliubov transformation. Both horizontal and vertical ladders contribute to the INS data, summing over different stripe domains. Thus we consider $\tilde{S}_{h,k}(\omega) = (S_{h,k}(\omega) + S_{k,h}(\omega))/2$. The constant-energy slices of $\tilde{S}_{h',k'}(\omega)$ shown in Fig. 3 [in the rotated frame of Fig. 1(c)] agree very well with the experimental results

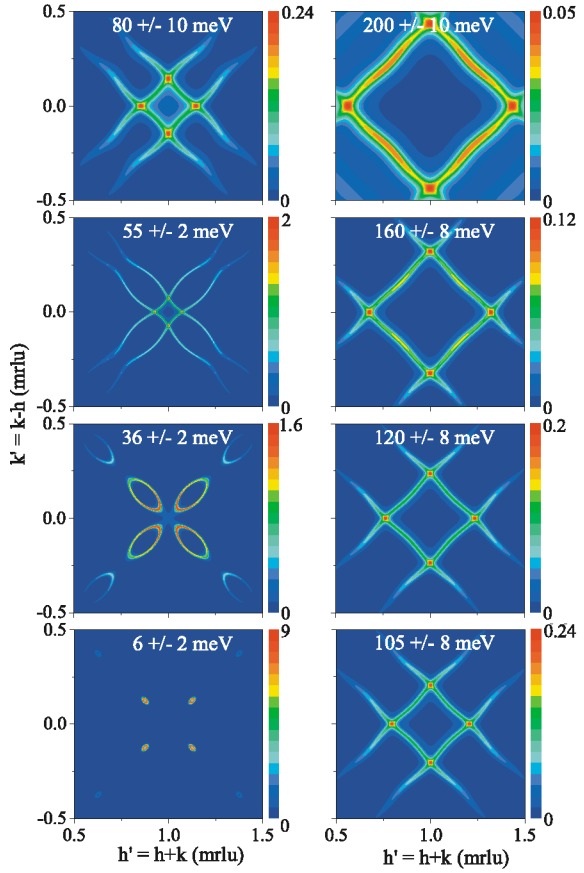


FIG. 3 (color). Constant-energy slices of $\tilde{S}_{h',k'}(\omega)$ for $J = 127$ meV, $J_{\rm cyc} = 0.2J$, and $J'/J = -0.072$ with $\omega \pm \Delta\omega$ given in each panel for direct comparison with Figure 2 in Ref. [10]. The experimental $\Delta\omega$ is accounted for by $\omega \rightarrow \omega + i\Delta\omega$ in (6).

[10]. At low energies (6 meV) the cones of magnons emerging from the superstructure satellites define a square around $\mathbf{Q}'_{\rm AF}$. The main intensity of these cones has shifted towards $\mathbf{Q}'_{\rm AF}$ at 36 meV, culminating in the resonance peak at the saddle point (44 meV). At still higher energies, the 1D character of the triplons of a quantum spin liquid predominates, giving rise to almost straight lines in the constant-energy slices. These lines form a diamond pattern which is rotated relative to the low-energy square.

The high-energy diamond is filled in the INS data, but not in our single-mode calculation. This discrepancy is caused by the finite experimental momentum resolution, by the decay of a single triplon (finite life time) into two or three triplons due to the interladder coupling, and by the missing two- and three-triplon channels of the isolated ladder (see above). The two-triplon weight piles up around $k = 1/2$ [18], which translates in 2D into a large contribution around $\mathbf{Q}_{\rm AF}$. Energetically, the lower edge of the three-triplon continuum is degenerate at $\mathbf{Q}_{\rm AF}$ with the one-triplon energy (e.g., for triplons with $q_1 = \mathbf{Q}_{\rm AF}$, $q_2 = -q_3 = (3/8, 1/2)$, and $\omega(q_2) = \omega(q_3) = 0$). Thus both channels contribute to the filling of the diamond.

For quantitative comparison we turn to the momentum-integrated structure factor $S(\omega)$. The one-triplon contribution is shown in Fig. 4(a). The saddle point gives rise to a logarithmic van Hove singularity which can be identified with the resonance peak observed in Ref. [10]. Qualitatively, pure spin wave calculations are similar in this respect [22]. A striking dependence of the singularity on $J_{\rm cyc}$ is found. Values of $J \approx 140$–$150$ meV (for $La_2CuO_4$) and $x_{\rm cyc} = 0.2$–$0.3$ are well established [15–17]. Using $x_{\rm cyc} = 0.2$ (0.25), we find $J = 127$ (162) meV from the INS resonance energy. This procedure fixes also the absolute scale of the intensity [Fig. 4(b)]. The quantitative agreement for the accepted exchange couplings strongly corroborates our approach. The remaining differences can be explained easily. (i) Our theory predicts a second sharp peak above 200 meV. There, the experimental resolution is only $\pm 20$–$25$ meV, so that the high-energy peak is washed out entirely [thin solid line in Fig. 4(b)]. (ii) We find too much weight below $\approx 40$ meV because we do not consider a finite staggered magnetization.

The superstructure periodicity of $4a$ with antiphase domain structure manifests itself in the reciprocal space coordinates of the satellites $(n/8, 1/2)$ and $(1/2, n/8)$ with $n$ odd. This order has been depicted either as *three-leg* ladders separated by a site-centered charge stripe or as the bond-centered charge stripes discussed here and in Ref. [10]. Recent *ab initio* results [13] support the bond-

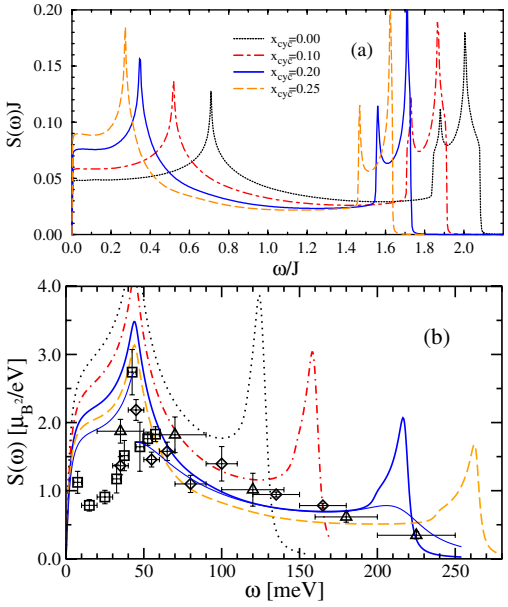


FIG. 4 (color online). (a) Momentum-integrated structure factor $S(\omega)$. (b) $S(\omega)$ integrated only over the magnetic Brillouin zone: Symbols: INS data from Ref. [10]. Lines: For each value of $x_{\rm cyc} = 0$, 0.1, 0.2, and 0.25 with $J'/J$ chosen to meet the quantum critical point (see text), we fix $J$ such that the lower singularity peaks at 44 meV ($J = 62$, 85, 127, and 162 meV). The intensity is not fitted but fixed by the value of $J$ (using a $g$ factor of $g = 2$). The broadening $\Delta\omega$ is set to 2.5 meV. Thin solid lines ($x_{\rm cyc} = 0.2$) mimic experimental details: (i) at high energies, Lorentzian broadening $\Delta\omega = 20$ meV; (ii) at low energies, integration only in the dotted region of Fig. 1(c) [30].

centered scenario. The quantitative agreement in Figs. 3 and 4 corroborates the two-leg ladder scenario, but coupled three-leg ladders cannot be ruled out at present.

Earlier, a unified description of the resonance peak and of the low-energy satellites was proposed based on strictly 1D models [23]. But in 1D the satellites carry much more spectral weight than the resonance. A true resonant behavior emerges only from a 2D saddle point.

In stripe-ordered $S = 1$ $La_{2-x}Sr_xNiO_4$ [24,25], isotropic magnons emerging from the superstructure satellites describe the INS data up to the highest measured energy ($\approx 100$ meV) [22]. In the nickelates, a spin wave picture is much more justified due to the larger spin $S = 1$ and due to the large interladder coupling $J'$, which was found to be $J'/J \approx 0.5$–$1$ [22,24,25]. This shifts the saddle point, where the magnon cones merge, to high energies. Indeed, enhanced intensity was observed at $\approx 80$ meV at $\mathbf{Q}_{\mathrm{AF}}$ [24]. In the cuprates, the saddle point is rather low due to the small $J'$ and the sizeable $J_{\mathrm{cyc}}$ [Fig. 4(a)].

Our spin-only model aims at the magnetic response of the stripe-ordered phase. However, INS data of twinned superconducting $YBCO_{6.6}$ [8] and of stripe-ordered $La_{15/8}Ba_{1/8}CuO_4$ [10] are stunningly similar. Since our model does not rely on long-range magnetic order, it is plausible that its qualitative features survive in the superconducting phase. The phase on the disordered side of the quantum critical point shows a spin gap [20], and we find good agreement [26] with the INS data of twinned $YBCO_{6.6}$ [8]. The downward dispersion below the resonance energy $\omega_r$ [5–9] as well as the upward dispersion above $\omega_r$ [6–9] are generic features of our model. However, there are two major shortcomings: (i) INS data of untwinned $YBCO_{6.85}$ [27] contradict the 1D geometry predicted for static stripes [26]. This may possibly be accounted for by, e.g., fluctuating stripes. (ii) Our spin-only model neglects charge degrees of freedom, which, e.g., cause a damping of the spin excitations. However, in stripe-ordered $La_{15/8}Ba_{1/8}CuO_4$ the spin-only model is applicable because the damping is reduced by charge order. Similarly, the appearance of the resonance peak and of the incommensurate low-energy modes below $T_c$ in YBCO [5,8] can be attributed to the vanishing damping if the resonance is lying below the particle-hole continuum. The absence of the resonance peak in LSCO, with similar $J$ but a smaller superconducting gap, suggests that the mode is located *within* the continuum, where it is overdamped [28,29]. The discussion of more detailed questions such as the doping dependence of $\omega_r$ would require to consider quantitative details of the effective interladder coupling and of the charge degrees of freedom.

In conclusion, we have given a unified description of low-energy 2D magnons, high-energy 1D triplons, and of the resonance mode at $\mathbf{Q}_{\mathrm{AF}}$ in stripe phases. Both the resonance energy and the spectral intensity agree quantitatively with the INS data of $La_{15/8}Ba_{1/8}CuO_4$ [10] for realistic values of $J \approx 130$–$160$ meV and $J_{\mathrm{cyc}}/J \approx 0.2$–$0.25$. This underlines the significance of quasi-1D quantum magnetism in the 2D cuprates.

We thank J. M. Tranquada for provision of the INS data and acknowledge fruitful discussions with M. Braden and the support by the DFG via SFB 608 and SP 1073.

*Note added.*—While we wrote this manuscript we became aware of a mean-field calculation of $\omega_{h,k}$ based on coupled dimers [31] leading to qualitatively similar results as in Fig. 3.

[1] A recent short review is given in Y. Sidis *et al.*, Phys. Status Solidi B **241**, 1204 (2004).
[2] For a recent review, see M. R. Norman and C. Pépin, Rep. Prog. Phys. **66**, 1547 (2003).
[3] J. M. Tranquada *et al.*, Nature (London) **375**, 561 (1995).
[4] H. B. Brom and J. Zaanen, in *Handbook of Magnetic Materials*, edited by K. H. J. Buschow (Elsevier, New York, 2003), Vol. 15, p. 379.
[5] P. Bourges *et al.*, Science **288**, 1234 (2000).
[6] D. Reznik *et al.*, Phys. Rev. Lett. **93**, 207003 (2004).
[7] M. Arai *et al.*, Phys. Rev. Lett. **83**, 608 (1999).
[8] S. M. Hayden *et al.*, Nature (London) **429**, 531 (2004).
[9] H. Mook *et al.*, Phys. Rev. Lett. **88**, 097004 (2002).
[10] J. M. Tranquada *et al.*, Nature (London) **429**, 534 (2004).
[11] E. Demler and S. C. Zhang, Nature (London) **396**, 733 (1998).
[12] K. P. Schmidt and G. S. Uhrig, Phys. Rev. Lett. **90**, 227204 (2003).
[13] V. I. Anisimov *et al.*, cond-mat/0402162 (2004).
[14] K. P. Schmidt, H. Monien, and G. S. Uhrig, Phys. Rev. B **67**, 184413 (2003).
[15] T. S. Nunner *et al.*, Phys. Rev. B **66**, 180404(R) (2002), and references therein.
[16] R. Coldea *et al.*, Phys. Rev. Lett. **86**, 5377 (2001).
[17] A. A. Katanin and A. P. Kampf, Phys. Rev. B **66**, 100403 (2002); Phys. Rev. B **67**, 100404 (2003).
[18] C. Knetter *et al.*, Phys. Rev. Lett. **87**, 167204 (2001).
[19] K. P. Schmidt, C. Knetter, and G. S. Uhrig, Acta Phys. Pol. B **34**, 1481 (2003).
[20] S. Sachdev, Science **288**, 475 (2000).
[21] S. D. Dalosto and J. Riera, Phys. Rev. B **62**, 928 (2000).
[22] F. Krüger and S. Scheidl, Phys. Rev. B **67**, 134512 (2003).
[23] C. D. Batista, G. Ortiz, and A. V. Balatsky, Phys. Rev. B **64**, 172508 (2001).
[24] P. Bourges *et al.*, Phys. Rev. Lett. **90**, 147203 (2003).
[25] A. T. Boothroyd *et al.*, Phys. Rev. B **67**, 100407(R) (2003).
[26] G. S. Uhrig, K. P. Schmidt, and M. Grüninger, J. Magn. Magn. Mater., "Magnetic excitations in the stripe phase of high-Tc superconductors" (to be published).
[27] V. Hinkov *et al.*, Nature (London) **430**, 650 (2004).
[28] D. K. Morr and D. Pines, Phys. Rev. Lett. **81**, 1086 (1998).
[29] Ar. Abanov and A. V. Chubukov, Phys. Rev. Lett. **83**, 1652 (1999).
[30] J. M. Tranquada (private communication).
[31] M. Vojta and T. Ulbricht, Phys. Rev. Lett. **93**, 127002 (2004).